APPLICATION OF OZONE ASSISTED MEMBRANE CLEANING FOR NATURAL ORGANIC MATTER FOULED MEMBRANES

Regina Khayrullina*[1], Chedly Tizaoui*[1], Paul Williams[1], Chris Spacie[2]

[1]: Centre for Water Advanced Technologies and Environmental Research, College of Engineering, Bay Campus, Swansea University, Swansea SA1 8EN, United Kingdom

[2]: Haydale Ltd, Clos Fferws Parc Hendre, Ammanford SA18 3BL, United Kingdom

*Correspondance: 803444@swansea.ac.uk; c.tizaoui@swansea.ac.uk

Keywords: PVDF; Graphene; Ozone; Membranes; Enhanced membranes; Membrane fouling; Natural organic matter; Membrane cleaning.

Abstract

The popularity of membrane technology in water treatment has been rising for over last 50 years due to wide range of filtration processes and applications, cost effective production and installation as well as safe and efficient water production. However, the development and improvement of membranes is ongoing due to number of weaknesses. Membrane fouling is a major drawback of membrane application in water and waste water treatment. Mostly caused by natural organic matter (NOM), fouling forms a layer on top of the membrane and blocks pores reducing the water permeation and can be potentially destructive to the membrane structure. The issue of membrane fouling can be addressed during membrane manufacturing, maintenance and operation. In the current study, the graphene-based nanomaterials (GBN) were incorporated in polyvinylidene fluoride (PVDF) to manufacture membranes via the phase-inversion technique. The resulting membranes show significant improvement to the properties of the pure PVDF membranes and their antifouling ability. The addition of GBN enhanced the water permeation by over 79% as a result of increased membrane hydrophilicity. Although this enhancement is beneficial, membrane fouling remained an issue despite the observed improvement. In this study, ozone, which is an effective oxidant, was

evaluated as a novel technique for the cleaning of humic acid-fouled membranes. When ozone cleaning was applied to the humic acid fouled membranes, reestablishment of close to original flux values was observed after just 30 minutes of cleaning. This statement is supported by SEM images that give an insight into the fouling of the membrane surface after the application of the cleaning methods. The data indicate that ozone is an effective technique for membrane cleaning against NOM induced fouling.

1 Introduction

Utilisation of membranes for water and waste water treatment has been a topic of great interest for over 50 years. Membrane filtration allows high efficiency and low cost production of purified water compared to the older less energy sustainable and expensive water treatment processes. The membrane processes can be classified in four main categories depending on pore size and rejection capability: microfiltration (MF), ultrafiltration (UF), nanofiltration (NF) and reverse osmosis (RO) (Sagle, 2004).Various types of membranes have been used for water treatment as well as other applications, ceramic, organo-mineral, metal or polymeric (Genné et al., 1997; Leiknes et al., 2004; Chatterjee and Kumar, 2007; Ebrahimi et al., 2010). Polymeric membranes are widely used in water purification areas such as desalination, waste water treatment and portable water treatment. The popularity of the polymeric membranes in water treatment is accounted for their superior properties such as high flexibility, fairly uncomplicated pore forming mechanism, low production cost and smaller imprint required for installation compared to inorganic material membranes (Yin and Deng, 2015).

Many researchers have invested their time and effort to improve various properties of membranes to achieve high quantity and quality of filtration along with long run life. These parameters can be jeopardised by membrane fouling which is a major drawback in membrane technology. Deposition of undesired particles on the surface and inside the pores of the membranes can affect the water permeation, solute rejection and degradation of the membrane materials resulting in reduced permeate quantity and quality (Van Geluwe et al., 2011). Membrane fouling, which can be reversible and/or irreversible can take one or more of the following forms: adsorption, pore blockage, gel formation and deposition (Field, 2010). Natural organic matter (NOM) has been proven to be the most common cause of fouling in membrane processes (Kweon and Lawler, 2005). Major constituents of NOM include polysaccharides, lipids, proteins, peptides, amino acids and humic substances which can in some cases account for 50% of NOM (Schmitt-Kopplin et al., 1999; Van

Geluwe et al., 2011). Application of ozone in presence of those substances causes their degradation to smaller molecules. It is typically conducted by rupture of double bonds in aromatic rings and reaction with electron donating groups for further oxidation and production of carbon dioxide. Small molecules such as aquatic peptides, proteins and amino acids degrade to carbonyl and carboxyl acids, nitrate and ammonia as well as interference with the folding ability of the proteins (Le Lacheur and Glaze, 1996; Sharma and Graham, 2010). Miao and Tao showed that ozonation of humic acid increased the presence of smaller constituents such as aromatics, ketones, aldehydes, alcohols and carboxylic acids which were further oxidised to produce esters and acids (Miao and Tao, 2008). Ozone serves as a very powerful oxidising agent with high reactivity due to the ozone molecule's electronic configuration and its resonance structure (Beltrán, 2004; Van Geluwe et al., 2011).

The ozone molecules electrophilic character originates from the positive formal charge of the central oxygen atom, while the negative charge on one of the terminal oxygen atoms contributes to ozone's nucleophilic character. The ozone reactions in water can vary from oxidation-reduction, dipolar cycloaddition or electrophilic substitutions. During these reactions free radicals (e.g hydroxyl radical, $^{\bullet}OH$) are formed, which are very reactive with most organic molecules. Therefore ozone reactions can be divided into direct reactions where ozone molecules react selectively with contaminants and indirect reactions where hydroxyl radicals produced during decomposition of ozone react with molecules in water (Beltrán, 2004). The hydroxyl radical reactions are non-selective and proceed with very high rates.

Removal of membrane surface fouling can be performed via physical, chemical or physicochemical cleaning methods. While reversible fouling can be eliminated by application of physical cleaning methods such as backflushing, irreversible can only be solved by chemical cleaning due to persistence of this type of fouling (José Miguel Arnal, (2011). Choice of chemical cleaning agent depends both on type of foulant and membrane material, so that the membrane doesn't get damaged

during the cleaning process. Chemicals such as sodium hydroxide, hypochlorite and hydrogen peroxide are widely used for effective membrane cleaning methods. However, these chemicals can cause damage to the membrane structure which in turn reduces the membrane efficiency and life time as well as causes secondary fouling (José Miguel Arnal, (2011).

Ozone assisted membrane cleaning is a novel technique for decomposition and removal of NOM induced fouling (Van Geluwe et al., 2011). Only recently, researchers have started investigating ozone treatment for membrane cleaning using various methods and membrane materials. Moslemi et al reported use of ozonation combined with ultrafiltration ceramic membranes for mitigation of membrane fouling (Moslemi et al., 2014). In addition Kim et al studied the effects of ozone backwashing applied in a metal membrane microfiltration system for fouling reduction(Kim et al., 2007). Due to growth of polymeric membrane applications it is essential to investigate efficient and effective cleaning methods for these membranes. However, little work has been done in combining polymeric membrane filtration and ozone cleaning. Although most organic membranes fail to withstand the ozone treatment, polymeric polyvinylidene fluoride (PVDF) membranes show high ozone resistance due to the high crystallinity of PVDF. As well as excellent ozone resistance, PVDF membranes exhibit good mechanical strength, thermal stability and chemical resistance (Liu et al., 2011).

In order to further increase the efficiency of the process, graphene-based nanomaterials (GBN) can be introduced in the modified PVDF membranes. A number of studies concentrate on incorporation of graphene oxide, reduced graphene oxide and carbon nanotubes in the membrane matrix (Choi et al., 2006; Lee et al., 2013; Zhao et al., 2014). It has been suggested that these nanomaterials increase membrane water permeability and mechanical strength as well as improve the antifouling properties (Liu et al., 2011; Lee et al., 2013; Suhartono and Tizaoui, 2015).

In this current work the emerging use of ozone assisted chemical cleaning of pure and GBN enhanced PVDF membranes was investigated. Using membrane characterisation and performance evaluation techniques, the efficiency of the membranes before and after modification as well as characterisation and mitigation of membrane fouling via cleaning studies was evaluated. Membrane cleaning studies involved utilisation of two different techniques: deionised water flushing and ozone assisted cleaning.

2 Experimental

2.1 Materials

PVDF Kynar polymer powder grade 761 and N-methyl-2-pyrrolidone (NMP) solvent 99%, extra pure (Sigma Aldrich, Dorset, UK) were used for membrane manufacturing. GBN have been kindly provided by Haydale Ltd, UK and used as membrane enhancing additives. The GBN planar particle size was 0.3-5 μm with thickness <50nm. Humic acid, technical grade used in this study, was taken as representation of natural organic matter and purchased from Sigma Aldrich, Dorset, UK.

2.2 Membrane preparation

Both pure and modified membranes were manufactured via a phase inversion method (Suhartono and Tizaoui, 2015). Briefly, dry PVDF powder was dissolved in NMP and stirred for 3 hours using a mechanical stirrer while maintaining the solution temperature at 65^{o}C in a water bath. After 3 hours, the mixture was cooled to room temperature and the membrane was then cast using a casting blade on a sheet of glass. The glass sheet with the cast membrane was immersed in deionised water at room temperature for 2 hours to ensure complete solvent-non-solvent displacement. For the GBN enhanced membranes the nanomaterials were first dispersed in NMP, and to increase the dispersion of nanoparticles the solution was sonicated in an ultrasonic bath.

2.3 Membrane Characterisation

The morphology of the manufactured membranes was characterised using optical and electronic microscopes. For general observation of the membrane surface and dispersion of the nanoparticles the Nikon Eclipse LV100ND optical microscope was used at various magnifications. For more detailed surface and cross section measurements the Hitachi S4800 Scanning Electron Microscope (SEM) was employed. The hydrophobicity of the manufactured membranes is typically investigated by measuring the water contact angles. In current experiment, the sessile drop method has been employed and recorded via a digital microscope with a camera, Supereyes B003+ K with Supereyes software. The samples were securely fixed on to a PVA sheet and exposed to a 2μL drop of deionised water at room temperature. The measurements were performed on different parts of the membrane to achieve reliable and repeatable results. Five measurements were made and the averages are reported here.

The membrane volume porosity was determined gravimetrically (Eq. 1).

$$\varepsilon(\%) = \frac{\left(m_{wet} - m_{dry}\right)/\rho_w}{\left(m_{wet} - m_{dry}\right)/\rho_w + m_{dry}/\rho_{PVDF}} \times 100 \quad \textit{(Eq 1)}$$

where m_{wet} is the mass of wet membrane (g), m_{dry} is the mass of dry membrane (g), ρ_w is the denisty of DI water (g/cm^3), ρ_{PVDF} is the density of the PVDF polymer (1.78 g/cm^3).

This calculation allows further investigation into the pore morphology of the membranes. The mean pore radius can be established by inputting the membrane volume porosity and filtration velocity in the Guerout-Elfor-Ferry equation (Yuliwati et al., 2011):

$$r_p = \sqrt{\frac{\left(2.9 - 1.75\varepsilon\right) \times 8\eta l Q}{\varepsilon A \Delta P}} \qquad \textit{(Eq2)}$$

where ε is the membrane volume porosity, η is the water viscosity (8.9 x 10^{-4} Pa s at 25°C), *l* is the membrane thickness (m), *Q* is the flowrate of the permeate (m^3/s), *A* is the membrane surface area (m^2), *ΔP* is the transmembrane pressure (Pa).

2.4 Performance

2.4.1 Flux

Membrane performance was tested using a cross flow filtration unit (CFU) where the permeation of deionised water through the membrane was measured. The experimental set up is displayed in Figure 1. The CFU operation conditions were set at a water flowrate of 1 L/min, a transmembrane pressure (TMP) 4.5 bar and all at room temperature 25±1°C. The membrane unit was assembled using a cellulose fibre support layer and a circular membrane of 36 mm diameter (active area of 10 cm^2). The permeate was collected over 20 minutes and recorded every 10 seconds using an electronic balance interfaced with a PC.

Figure 1

2.4.2 Humic acid rejection

Membrane performance was further investigated via the ability of the membranes to reject humic acid (HA). The humic solution was prepared at 0.05g/L humic acid and stirred for 24 hrs without pH

adjustment at pH 6. Using the CFU set up at flow rate 1L/min and TMP 4.5 bar, the membranes were employed to filtrate the humic acid solution until the permeate volume reached 200mL.

The permeate was collected every 5-10mL and analysed via UV-vis spectrophotometer (Agilent, HP 8453) at specific to humic acid wavelength 254nm (Xu et al., 2013).

2.4.3 Fouling study

Rapid fouling of the membranes was made by employment of a dead end filtration system. The dead end filtration (DEF) testing operation was performed at a pressure 3.5 bar for a period of 2 hours using a HA solution at a concentration 1 g/L and pH of approximately 6. Prior to and after the fouling testing, the membranes were subjected to pure water flux measurements to quantify the fouling efficiency.

2.5 Membrane cleaning

In this study two types of membrane cleaning were used. The first was based on an ozone solution and the other was based on regular deionised water forward flushing. To be able to perform the cleaning, the membranes were first exposed to fouling tests with the DEF set-up. The HA fouled membranes were then transferred and assembled in the CFU membrane unit. Ozone in oxygen was supplied to the feed tank via a frit glass gas diffuser placed at the centre of the tank of the CFU (Figure 1). The ozone was generated by a BMT 803 ozone generator (BMT Messtechnik, Germany) and the gas phase ozone concentration was measured by a BMT 963 ozone analyser. Approximately 3 L of deionised water at room temperature and approximate pH 6 was used for the cleaning study.

The concentration of dissolved ozone was measured by UV-vis spectrophotometer (Agilent, HP 8453) at a wavelength 260 nm at the start and end of the membrane treatment(Von Sonntag and Von Gunten, 2012). The values of dissolved ozone concentrations were set by setting the ozone gas concentration supplied by the O_3 generator at aproximately 50 g/m^3 NTP. The membrane cleaning was performed for 30 minutes with constant ozonation of water in the tank and at flow rate of the

ozonated solution of 1L/min. The second method involved a similar set up to flux measurement where 3 L of ozone-free deionised water was used to flush the membrane for 30 minutes.

The permeation rates were recorded in a similar fashion as the pure water flux measurements. The permeate for both cleaning techniques was characterised using UV-vis absorption at 254 nm (UV_{254}). In order to remove residual ozone from the permeate, a small amount of sodium thiosulfate was added immediately to the sample before taking the measurement with the UV-vis spectrophotometer.

3 Results and discussion

3.1 Membrane characterisation

3.1.1 Membrane morphology

Microscopic images of the two membranes are shown in Figure 2 for the pure PVDF membrane (Figure 2(a)) and for the graphene-based nanomaterials enhanced membrane (Figure 2(b)) where the nanoparticles can be seen embedded in the polymer matrix. The SEM images provide better insight into the surface and the pore morphology of the membranes presented in Figure 3. The images show the pore network of both membranes where the pure PVDF membrane shows more uniform pore size and distribution whilst the GBN-PVDF membranes show more irregular porous structure with graphene nanoparticles imbedded in the pores.

Figure 2

Figure 3

Figure 4 shows the values of the volume porosity and mean pore radius of pure- and GBN- PVDF membarnes. The volume porosity of the pure PVDF membrane is 80.8% while the value for the GBN PVDF is slightly higher at 82.4%. As well as an increase in porosity with the addition of GBN, the mean pore radius also rises by about 2 nm. Impregnation of PVDF membranes with GBN is likely to cause changes in the membrane pore network by increasing the porosity and mean radius of the pores which in turn affects the membrane permeation properties.

Figure 4

3.1.2 Contact angle

Contact angle (CA) measurements provide an estimated wettability of the membranes. High CA represents membranes with high hydrophobicity, meaning the wettability is low. The average CA of the pure PVDF membranes is around 63.1° while GBN membranes have a CA of average value of 54.4°. The incorporation of GBN has hence resulted in approximately 16% reduction in membrane CA and therefore the wettability of the membrane has also increased. Such reduction in CA also supports the increased permeation values obtained for GBN-PVDF membranes as they become more hydrophilic. Reduction in contact angles also affects the antifouling properties of the membranes. The hydrophilicity of the membranes affects the interactions between the membrane surface and the foulants present in water, leading to lower sorption of contaminants within the membrane(Wang et al., 2012)

Figure 5

3.2 Membrane performance

3.2.1 Pure water flux and permeation:

Figure 6 represents pure water flux and permeability of the pure and GBN enhanced PVDF membranes. As can be seen in Figure 5, the incorporation of GBN enhanced membrane permeation when compared to the pure PVDF membrane. The graph shows membrane flux values of GBN-PVDF at 126.1 L/m^2.h.bar (st. dev. 11.3 L/m^2.h.bar) and the pure PVDF at 70.3 L/m^2.h.bar (st. dev. 6.7 L/m^2.h.bar). GBN addition increased the PVDF membrane permeation by over 79%. This is likely due to the increased pore size of GBN-PVDF membrane.

Figure 6

3.2.2 Humic acid rejection

The rejection data was divided into initial, average 10-40mL and average 40-200mL. Figure 7 shows that the rejection for both membranes improves with permeation volume where after 40mL of permeate the rejection exceeded 90%.

Figure 7

Figure 7(b) provides a close view of the rejection efficiency representation for the membranes. The initial rejection of the graphene enhanced membrane has proven to be slightly higher than that of pure PVDF membrane. The same trend can be seen in the 40-200mL permeate humic acid rejection.

3.2.3 Anti-fouling ability

If a membrane has higher antifouling properties this will prevent the accumulation of foulants and pore blockage. According to Figure 8, the fouling of the pure PVDF membrane appears to be more rapid with a drastic reduction of the membrane flux whilst the GBN enhanced membrane has less of a reduction of flux which probably indicates less fouling. The data suggests that GBN enhancement provides better antifouling properties due to the higher hydrophilicity of the membrane as shown by the contact angle measurements.

Figure 8

3.3 Cleaning studies:

3.3.1 Water flushing

In order to evaluate the efficiency of ozone assisted cleaning, the forward pure water flushing in cross flow setup was used to compare the results. Prior to any fouling or cleaning, the membranes were subjected to pure water flux (PWF) measurement as a benchmark for further comparison. The PWF measurements are shown in Figure 9 for pure PVDF and GBN-PVDF membranes (blue lines). The PWF was measured via CFU with a cross flow rate of 1 L/min and a transmembrane pressure of 4.5 bar for 20 minutes. The membranes have then been fouled using DEF at 1 g/L HA solution at 3.5 bar pressure for 2 hours until the fouled flux became stable. The fouled membranes were again tested

for PWF to establish the effect of fouling. Figure 9 (red lines) shows a reduction in PWF after fouling the membrane. Linearity of the graphs serves as an indication that the cleaning technique involving only DI water does not influence the flux and provides only minimal or no removal of membrane fouling. The comparison of forward flushing of the two membranes is represented in Figure 10. The results show that the membrane flux was reduced by 110% for pure PVDF and 77.4% for the GBN enhanced due to the HA membrane fouling. In addition, the PWF of the fouled GBN-PVDF is almost as high as the unfouled pure PVDF membrane. This improvement in antifouling can be accredited to the enhanced membrane hydrophilicity due to GBN addition.

Figure 9

Figure 10

3.3.2 Ozone cleaning

Humic acid fouled membranes were exposed to ozone solutions in the same fashion as the water flushing experiments. The effect of ozone cleaning is shown in Figure 11 for pure PVDF and GBN-PVDF membranes. Figure 11 shows continuous enhancement of the water flux as the membrane was exposed to the ozone solution indicating the removal of the fouling originally retained by the membrane. Initially (red part shown in the curve), the flux was approximated at about 38.4 and 50 $L/m^2.h$ for pure PVDF and GBN-PVDF respectively and by the end of the cleaning process with the ozone solution (after about 25 min), the flux reached the values 82.6 and 117.3 $L/m^2.h$ for pure PVDF and GBN-PVDF respectively. These flux values match those of the fresh unfouled membranes (Figure 9 – blue lines). Hence ozone treatment provides close reestablishment of the original fluxes of both membranes which indicates that ozone is an effective membrane cleaning agent. This can be explained by the removal of the surface cake layer retained by the membrane and

elimination of possible pore blockages due to HA rejection (Figure 12 and 13). As can be seen in Figure 12(c) and 13(d), the membrane surface became fully clean and the pores do not show signs of blockage as exhibited by the SEM image. Similar results were also obtained for the GBN-PVDF membranes (Figures 14 and 15).

Figure 11

Figure 12

Figure 13

Figure 14

Figure 15

4 Conclusion

This study shows that ozone was effective in cleaning humic acid fouled PVDF membranes. The data shows that ozone cleaning achieves close recovery to the membranes original permeation and flux values to while the forward flushing with DI water provided only limited removal of fouling.

In addition, the enhancement of PVDF membranes with carbon based nanomaterials via the phase inversion method proved to be beneficial for the membrane performance and antifouling properties. This is shown by:

- Improvement of permeation and pure water flux by approximately 79% as well as exhibiting higher porosity and mean pore radius.
- Reduction of contact angle measurements by 16% indicating an increase in hydrophilicity of the modified membranes which benefits the membrane permeation properties.
- Superior antifouling properties compared to the pure PVDF membranes due to improved hydrophilicity.

Considering the beneficial enhancement of the PVDF membrane properties further investigation of the effects of carbon based nanomaterials to achieve even greater membrane properties is warranted.

Acknowledgement

We acknowledge the financial support of Knowledge Economy Skills Scholarships (KESS). KESS is a pan-Wales higher level skills initiative led by Bangor University on behalf of the HE sector in Wales. It is partly funded by the Welsh Government's European Social Fund (ESF) convergence programme for West Wales and the Valleys.

References

Beltrán, F.J., Ozone reaction kinetics for water and wastewater systems Boca Raton, 2004)
Chatterjee, S., and V. Kumar. 2007. "Polymeric Membranes used for Water Purification", Popular Plastics & Packaging 52(12): 64-67.

Choi, J.-H., J. Jegal, and W.-N. Kim. 2006. "Fabrication and characterization of multi-walled carbon nanotubes/polymer blend membranes", Journal of Membrane Science 284(1): 406-415.
Ebrahimi, M., D. Willershausen, K.S. Ashaghi, L. Engel, L. Placido, P. Mund, P. Bolduan, and P. Czermak. 2010. "Investigations on the use of different ceramic membranes for efficient oil-field produced water treatment", Desalination 250(3): 991-996.
Field, R., Fundamentals of Fouling, in Membrane Technology. Wiley-VCH Verlag GmbH & Co. KGaA, pp. 1-23 (2010).
Genné, I., W. Doyen, W. Adriansens, and R. Leysen. 1997. "Organo-mineral ultrafiltration membranes", Filtration & Separation 34(9): 964-966.
José Miguel Arnal, B.G.a.-F.a.M.a.S. (2011. "Membrane Cleaning", Expanding Issues in Desalination:
Kim, J.-O., J.-T. Jung, I.-T. Yeom, and G.-H. Aoh. 2007. "Effect of fouling reduction by ozone backwashing in a microfiltration system with advanced new membrane material", Desalination 202(1): 361-368.
Kweon, J.H., and D.F. Lawler. 2005. "Investigation of membrane fouling in ultrafiltration using model organic compounds", Water Science and Technology 51(6-7): 101-106.
Le Lacheur, R.M., and W.H. Glaze. 1996. "Reactions of Ozone and Hydroxyl Radicals with Serine", Environmental Science & Technology 30(4): 1072-1080.
Lee, J., H.-R. Chae, Y.J. Won, K. Lee, C.-H. Lee, H.H. Lee, I.-C. Kim, and J.-m. Lee. 2013. "Graphene oxide nanoplatelets composite membrane with hydrophilic and antifouling properties for wastewater treatment", Journal of membrane science 448: 223-230.
Leiknes, T., H. Ødegaard, and H. Myklebust. 2004. "Removal of natural organic matter (NOM) in drinking water treatment by coagulation–microfiltration using metal membranes", Journal of Membrane Science 242(1–2): 47-55.
Liu, F., N.A. Hashim, Y. Liu, M.R.M. Abed, and K. Li. 2011. "Progress in the production and modification of PVDF membranes", Journal of Membrane Science 375(1–2): 1-27.
Miao, H., and W. Tao. 2008. "Ozonation of humic acid in water", Journal of Chemical Technology & Biotechnology 83(3): 336-344.
Moslemi, M., S.H. Davies, and S.J. Masten. 2014. "Hybrid ozonation–ultrafiltration: The formation of bromate in waters containing natural organic matter", Separation and Purification Technology 125: 202-207.
Sagle, A., and B. Freeman. 2004. ""Fundamentals of Membranes for Water Treatment,"", The Future of Desalination in Texas Volume 2(Report Number 363): 137-154
Schmitt-Kopplin, P., D. Freitag, A. Kettrup, N. Hertkorn, U. Schoen, R. Klöcking, B. Helbig, F. Andreux, and A. Garrison, W. 1999. "Analysis of synthetic humic substances for medical and environmental applications by capillary zone electrophoresis", Analusis 27(5): 390-395.
Sharma, V.K., and N.J.D. Graham. 2010. "Oxidation of Amino Acids, Peptides and Proteins by Ozone: A Review", Ozone: Science & Engineering 32(2): 81-90.
Suhartono, J., and C. Tizaoui. 2015. "Polyvinylidene fluoride membranes impregnated at optimised content of pristine and functionalised multi-walled carbon nanotubes for improved water permeation, solute rejection and mechanical properties", Separation and Purification Technology 154: 290-300.
Van Geluwe, S., L. Braeken, and B. Van der Bruggen. 2011. "Ozone oxidation for the alleviation of membrane fouling by natural organic matter: A review", Water Research 45(12): 3551-3570.
Von Sonntag, C., and U. Von Gunten, Chemistry of ozone in water and wastewater treatment IWA publishing, 2012)
Wang, Z., H. Yu, J. Xia, F. Zhang, F. Li, Y. Xia, and Y. Li. 2012. "Novel GO-blended PVDF ultrafiltration membranes", Desalination 299: 50-54.
Xu, J., J. Wu, and Y. He, Functions of natural organic matter in changing environment Springer Science & Business Media, 2013)
Yin, J., and B. Deng. 2015. "Polymer-matrix nanocomposite membranes for water treatment", Journal of Membrane Science 479: 256-275.

401 Yuliwati, E., A.F. Ismail, T. Matsuura, M.A. Kassim, and M.S. Abdullah. 2011. "Characterization of surface-
402 modified porous PVDF hollow fibers for refinery wastewater treatment using microscopic
403 observation", Desalination 283: 206-213.
404 Zhao, C., X. Xu, J. Chen, G. Wang, and F. Yang. 2014. "Highly effective antifouling performance of
405 PVDF/graphene oxide composite membrane in membrane bioreactor (MBR) system", Desalination
406 340: 59-66.

407

Figures

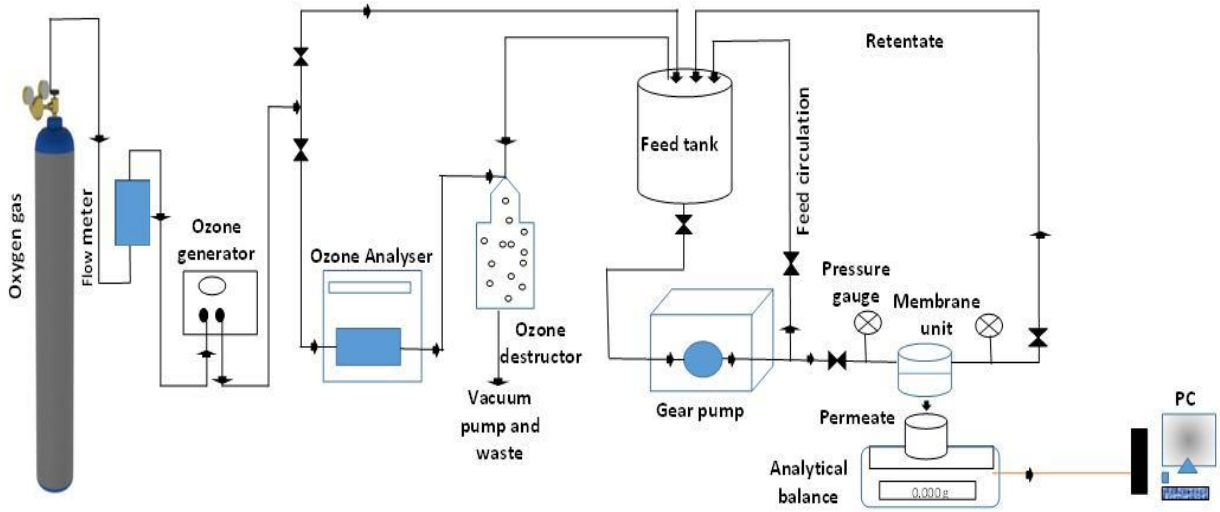

Figure 1: Hybrid membrane/ozone system for membrane cleaning.

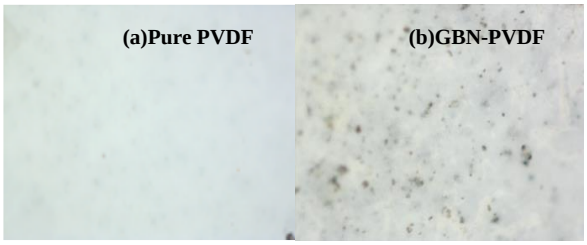

Figure 2 Digital images of (a) pure PVDF (b) GBN-PVDF membranes. Magnification x60

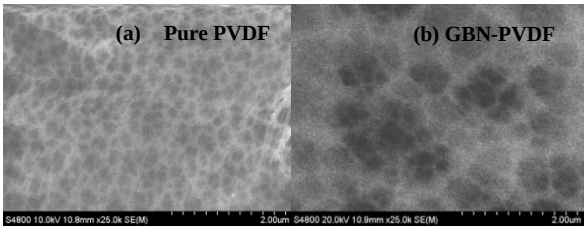

Figure 3 SEM images of (a) pure PVDF (b) GBN-PVDF membranes. Magnification x25K.

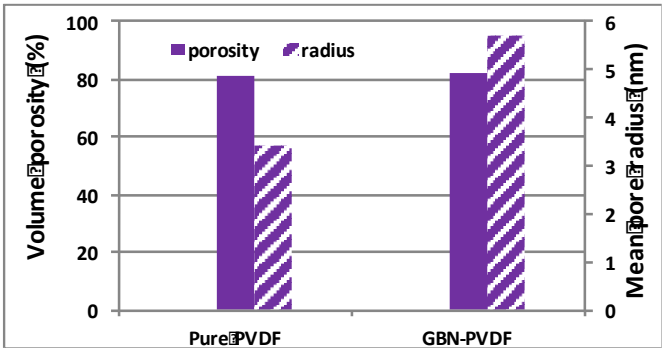

Figure 4 Volume porosity and mean pore radius values of membranes

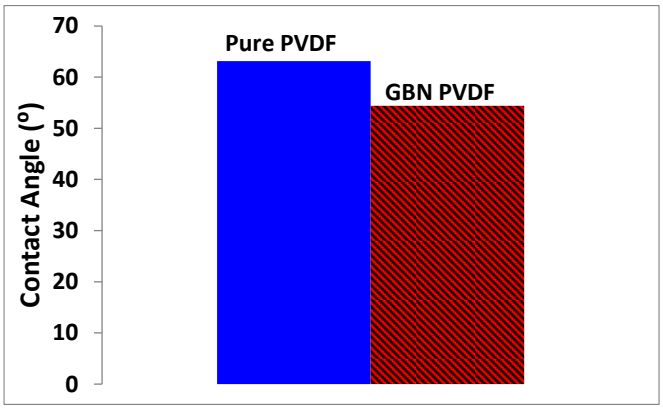

Figure 5 Contact angle data for pure PVDF and GBN-PVDF membranes.

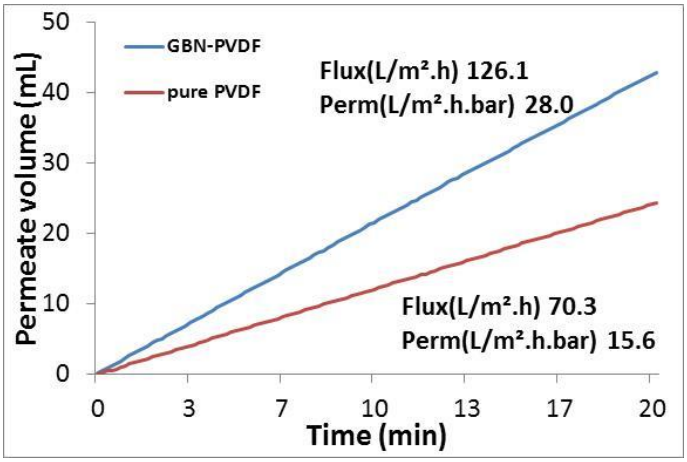

Figure 6 Pure water flux and permeation measurements of both pure PVDF and GBN-PVDF membranes Flow rate - 1L/min, TMP - 4.5 bar, at room temperature.

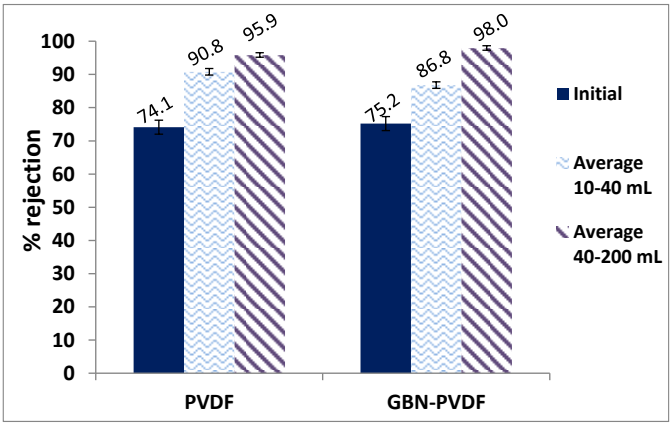

Figure 7 Rejection efficiency of the membranes. Humic acid concentration – 0.05g/L, pH aprox. 6, flow rate – 1L/min, pressure -4.5 bar, at room temperature. UV-vis wavelength 254.

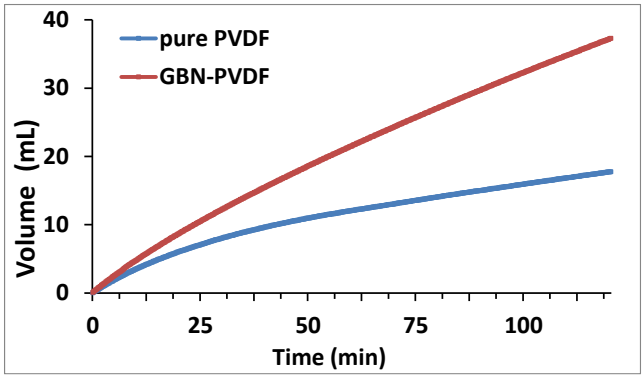

Figure 8 Humic acid fouling of pure and GBN enhanced PVDF membranes (dead end filtration). Humic acid concentration 1g/L, pressure - 3.5 bar, time 120 mins, at room temperature.

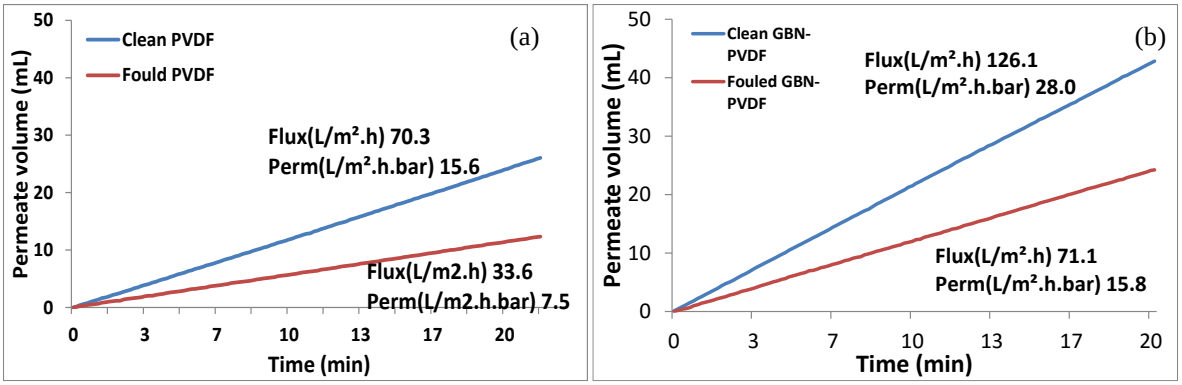

Figure 9 PWF and permeation of (a) pure PVDF and (b)GBN-PVDF membranes. Flow rate - 1L/min, TMP - 4.5 bar, at room temperature.

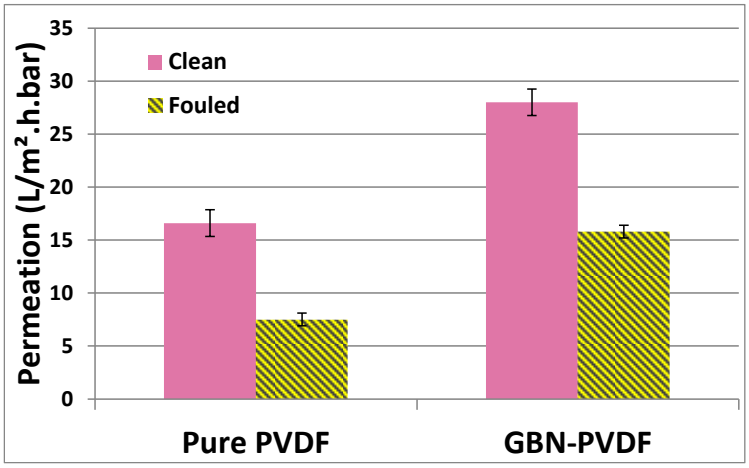

Figure 10 Pure water flushing. Flow rate - 1L/min, TMP - 4.5 bar, at room temperature.

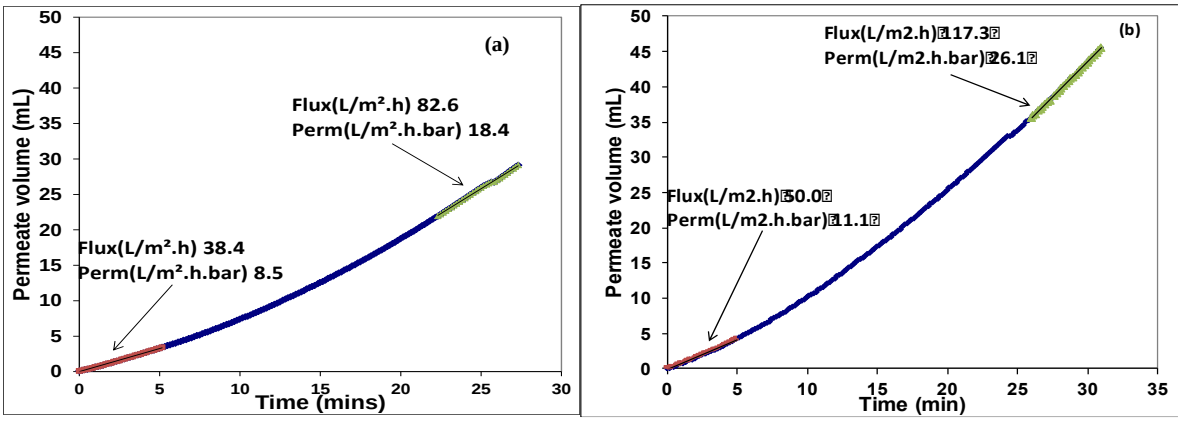

Figure 11 Ozone cleaning of fouled membranes (a) Pure PVDF, (b) GBN-PVDF ozone cleaning. Liquid ozone concentration = approx. 3 mg/L, flow rate - 1L/min, TMP - 4.5 bar, at room temperature.

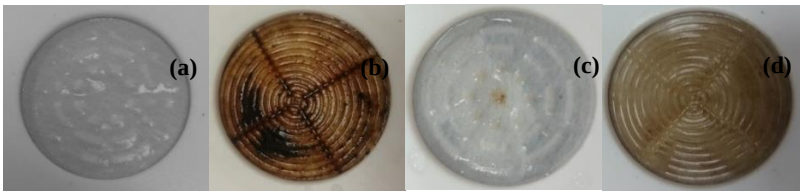

Figure 12 Photos of pure-PVDF membranes (a) initial, (b) fouled, (c) O_3 cleaned, (d)H_2O cleaned

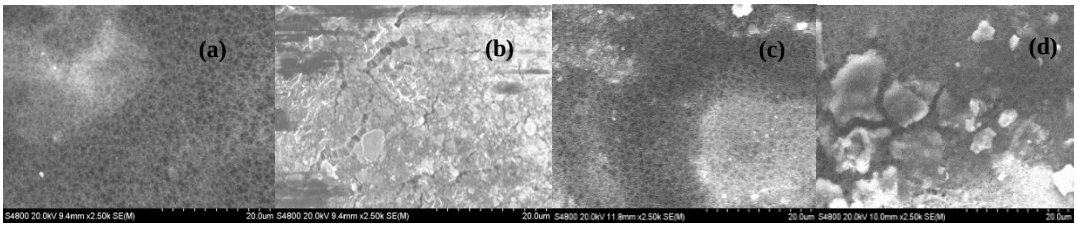

Figure 13 SEM of pure-PVDF membranes (a) initial, (b) fouled, (c) O_3 cleaned, (d)H_2O cleaned

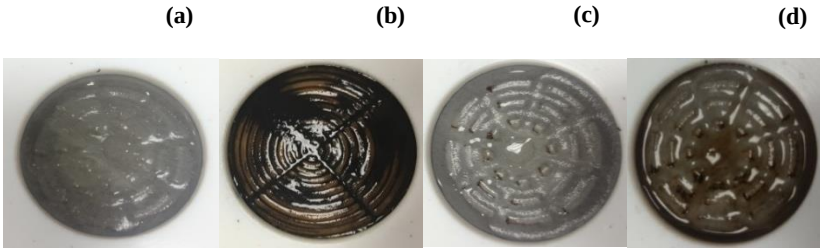

Figure 14 Photos of GBN-PVDF membranes (a) initial, (b) fouled, (c)O_3 cleaned, (d)H_2O cleaned

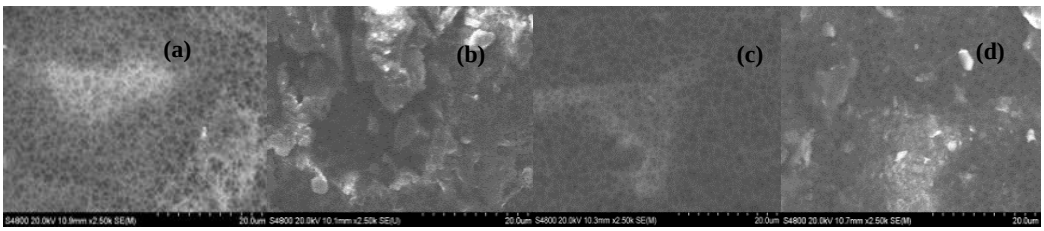

Figure 15 SEM images of GBN-PVDF membranes magnification 2,500x (a)initial, (b) fouled, (c)O_3 cleaned, (c)H_2O cleaned